University of Basel

– Master Thesis FS 2012 –

Precrystallization screen of Na^+/Ca^{2+} exchangers from thermophilic organisms

---

Author: Nicolas Devantay

Submitted to: Prof. Dr. Henning Stahlberg

Supervisor: Dr. Mark Hilge

Basel, July 6, 2012

Abstract

Together with the sarcoplasmic Ca^{2+} ATPase (SERCA) the Na^+/Ca^{2+} exchanger (NCX) is the major Ca^{2+} extrusion mechanism in the heart. Despite its paramount importance structural information on NCX is still very limited. In view of the challenges associated with membrane protein structure determination we focused on less complex bacterial NCX homologs, in particular on exchangers from thermophilic organisms. Using an efficient ligation-independent cloning approach we prepared ten thermophilic exchangers in form of GFP-fusions for expression in *Pichia pastoris*. In-gel fluorescence analysis revealed for three exchangers suitable expression levels for structural studies. Subsequently, the promising candidates were extracted with three to five different detergents and their monodispersity was tested using Fluorescence Size-Exclusion Chromatography (FSEC). For two exchangers, *Thermotoga maritima* and *Deinococcus radiodurans*, suitable detergents could be found and an efficient purification protocol was established. Thereby, optimized purification tags were developed that will be beneficial for other future projects.

Contents

1. Introduction

1.1. Ca^{2+} homeostasis

Dramatic differences in Ca^{2+} concentrations of the extracellular space (approximately 2mM) and intracellular Ca^{2+} stores, the endoplasmic reticulum (ER) and mitochondria, compared to the Ca^{2+} concentrations in the cytosol (approximately 100nM) create optimal conditions for Ca^{2+} to function as an essential messenger within prokaryotic and eukaryotic cells. There, Ca^{2+} plays crucial roles in processes such as signal transduction, exocytosis, contraction, metabolism, transcription, and fertilization by reversibly interacting with a large number of ligands. To accomplish these divers tasks Ca^{2+} is spatially and temporally tightly controlled by Ca^{2+} transporters that either import Ca^{2+} into the cytosol or export Ca^{2+} from the cell or back into the intracellular Ca^{2+} stores. This set of Ca^{2+} transporters is generally referred to as Ca^{2+} signaling toolkit [1].

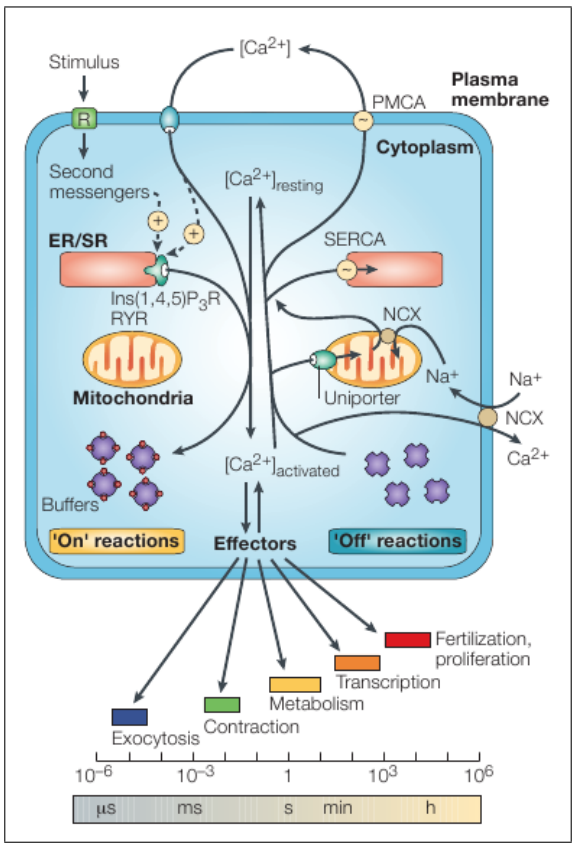

Figure 1: Overview of Ca^{2+} signaling dynamics and homeostasis from Berridge *et al.*, divided in "on" and "off" reactions. Ca^{2+} binding to effectors generally activates cellular processes while removal of Ca^{2+} deactivates them. Most of the intracellular Ca^{2+} (red spheres) is bound to buffers. Internal Ca^{2+} stores such as the endoplasmic/sarcoplasmic reticulum (ER/SR) and mitochondria have Ca^{2+} concentrations between 0.5-1mM. Compared to the Ca^{2+} concentrations of the extracellular space and the internal stores, the Ca^{2+} concentration in the cytosol is approximately 10'000-fold lower [2].

In cardiomyocytes e.g., Ca^{2+} enters the cytosol *via* L-type Ca^{2+} channels such as the dihydropyridine receptor. Thereby, the initial Ca^{2+} triggers Ca^{2+} release by the ryanodine receptor in the ER. To maintain the cytosolic Ca^{2+} concentrations at around 100nM, Ca^{2+} released to the cytosol has to be removed again. This task is performed by the plasma membrane Na^+/Ca^{2+} exchanger (NCX) and the Ca^{2+} ATPases in the ER and the plasma membrane, SERCA and PMCA, respectively. In addition, Ca^{2+} can also be removed from the cytosol *via* the recently identified Ca^{2+} uniporter that is located in the inner mitochondrial membrane. An overview of the Ca^{2+} signaling dynamics and homeostasis is presented in Fig. 1.

1.2. Mammalian NCX

In mammals bulk amounts of Ca^{2+} are removed from the cell by NCX that expels one Ca^{2+} ion for the uptake of three Na^+ ions. Using the Na^+ gradient established by the Na^+/K^+ ATPase, NCX executes 2500-5000 turnovers per second and molecule. As a member of the Cation/Ca^{2+} superfamily [3] NCX exists in three isoforms, NCX1 [4], NCX2 [5], and NCX3 [6] that show about 70% sequence identity among each other. In addition, numerous splice variants have been described for NCX1 [7, 8] and NCX3 [9].

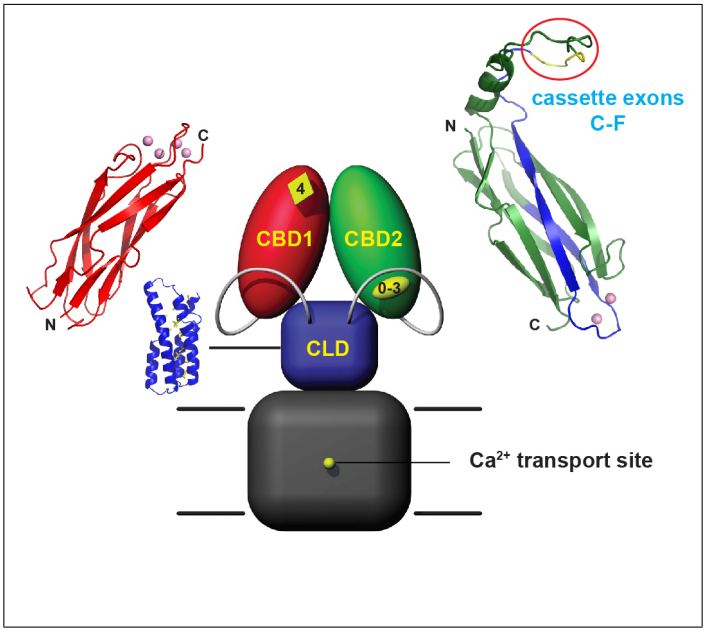

Figure 2: Hypothetical model of NCX that consists of CBD1 (red), CBD2 (green), CLD (blue), and the TM (grey). Ca^{2+} initially binds to CBD1 and only at concentrations above 1μM to CBD2. For sustained Na^+/Ca^{2+} exchange Ca^{2+} binding to CBD2 is required. In NCX1, Ca^{2+} binding properties of the CBD2 Ca^{2+} binding sites strongly depend on the mutually-exclusive exon A or B depicted in blue, while residues encoded by the small cassette exons influence affinities of the CBD1 Ca^{2+} binding sites [10].

Structurally, NCX probably consists of four domains (Fig. 2): a transmembrane domain (TM; in case of NCX1.4 residues 1-217 and 727-912), a domain that shows homology with α-

catenin (catenin-like domain or CLD), and two Ca^{2+} binding domains referred to as CBD1 and CBD2 [11]. The CBDs function as Ca^{2+} sensors for the Ca^{2+} concentration in the cytosol and regulate ion transport by NCX. Generally, Ca^{2+} first binds with high affinity (100-600nM) to CBD1 and thereby induces Na^+/Ca^{2+} exchange [12]. To maintain ion transport by NCX Ca^{2+} has to also bind to CBD2. Interestingly, variation in CBD2 as a consequence of alternative splicing modulates exchange properties of NCX. For instance, in excitable cells where high Ca^{2+} fluxes are needed, NCX1 variants are only encoded by the mutually-exclusive exon A, while in non-excitable cells splice variants are based on exon B. Structural analysis revealed that only exon A encoded variants are capable of Ca^{2+} binding to CBD2 [11]. In contrast, residues encoded by the small cassette exons C-F at the opposite end of CBD2 influence Ca^{2+} affinities of the Ca^{2+} binding sites in CBD1. Finally, these Ca^{2+} binding and release events are relayed *via* the CLD to the TM, thereby permitting and denying access of Na^+ and Ca^{2+} ions to the transport binding sites.

1.3. Phylogenetic classification of Cation/Ca^{2+} exchangers

Cation/Ca^{2+} exchangers are found in organisms ranging from bacteria to humans and are classified into five branches, YRBG, CAX, NCX, NCKX, and CCX [3]. The YRBG branch includes sequences of H^+/Ca^{2+} exchangers of bacterial and archaeal origin. Otherwise similar to YRBG the CAX branch in addition contains representatives from fungi and plants that commonly exchange three protons for one Ca^{2+} ion. The NCKX branch features an additional K^+-dependency and exchanges four Na^+ ions for the uptake of one Ca^{2+} and one K^+ ion, presumably to compensate for an insufficient Na^+ gradient in certain cells. Like H^+/Ca^{2+} exchangers NCKX lack the regulatory CBDs and generally operate slower than members of the NCX family [3]. Finally, the CCX branch consists of a single member, designated as NCKX6. Uniquely, NCKX6 is not only capable of Na^+/Ca^{2+} exchange with and without K^+, but it can also exchange Ca^{2+} for Li^+ ions. Furthermore, in 2010, NCKX6 was identified as the long sought mitochondrial Na^+/Ca^{2+} exchanger. With respect to the counter ions, bacteria, archaea, and plants predominantly exchange protons for Ca^{2+} as these organism mostly possess H^+ gradients. In contrast, animals generally express NCX and NCKX at the plasma membrane due to their Na^+ gradient and H^+/Ca^{2+} exchangers in organelles such as the vacuole. Sequence identities between the members of the five Cation/Ca^{2+} exchanger branches are generally well below 20% and alignments are based on two conserved regions referred to as α-repeats. As probably all members of the Cation/Ca^{2+} exchanger superfamily originate from an ancient gene duplication event [13, 3, 14] these α-repeat regions were until recently believed to form oppositely oriented re-entrant loops that were suggested to be involved in ion binding and translocation [13, 15]. Extensive mutational studies of the α-repeat regions for *canis* NCX1 revealed for most of the highly conserved residues functions in ion binding or structural roles.

1.4. Structure of a bacterial NCX homolog from *Methanococcus jannaschii* (NCX_Mj)

A recent major development in the understanding of Na^+/Ca^{2+} exchange was the determination of the structure of a prokaryotic homolog for the TM of NCX from *Methanococcus jannaschii* [16]. Remarkably, despite its archaeal origin, NCX_Mj was demonstrated to rather be a Na^+/Ca^{2+} than a H^+/Ca^{2+} exchanger. The 1.9Å crystal structure revealed a largely symmetrical transmembrane domain, arranged in form of two structurally similar halves of five α-helices with opposite topology. Helices 2 to 5 and 7 to 10 are tightly packed whereas helices 1 and 6 are somewhat separated from the bundle and tilted at an angle of approximately 45° with respect to the vertical axis of the membrane.

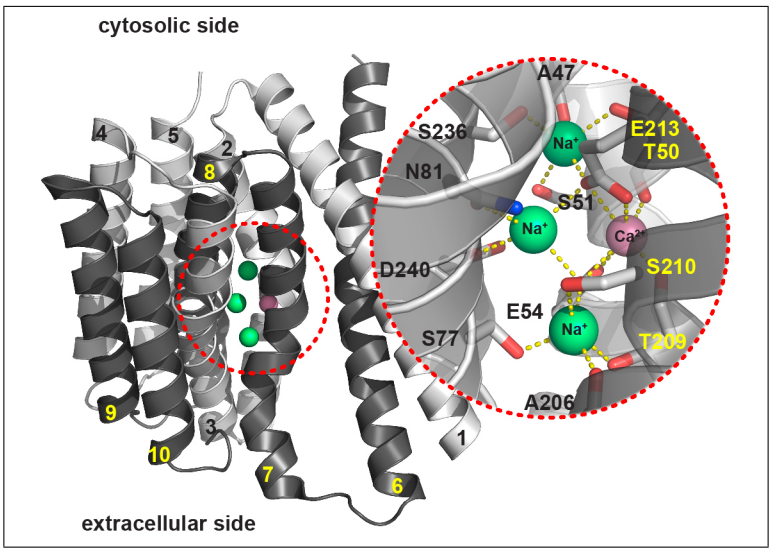

Figure 3: Structure of the NCX homolog from *Methanococcus jannaschii* NCX_Mj (PDB code: 3V5U), displaying symmetry-related helices 1-5 (light grey) and 6-10 (dark grey). The inset shows the detailed coordination of one Ca^{2+} and three Na^+ ions (Figure taken from [10]).

In line with the proposed transport stoichiometry of one Ca^{2+} ion in exchange for three Na^+ ions, four cation binding sites, one specific for Ca^{2+} and three that probably bind Na^+, were identified in the protein core at the center of the membrane. Strikingly, all residues participating in ion binding are highly conserved in the NCX and NCKX branches of the cation/Ca^{2+} exchanger superfamily [3]. In particular, in the center Glu54 (Glu113 in canine NCX1) and Glu213 (Asp814) coordinate the Ca^{2+} ion *via* their carboxylate groups, while the backbone carbonyl oxygen atoms of Thr50 and Thr209 complement the binding site. In addition, the OE2 of Glu54 and Glu213 contribute to the middle Na^+ binding site as well as to the Na^+ binding sites towards the extra- and intracellular side, respectively. The latter two Na^+ binding sites share identical ligand chemistry and geometry where Ser77, Ala206, Thr209, and S210 form the Na^+ binding site oriented towards the extracellular side and Ala47, Thr50, Ser51, and Ser236 constitute the Na^+ binding site closer to the intracellular side. Finally, Asn81

and Asp240 complete the coordination scheme of the middle Na^+ binding site.

1.5. Membrane proteins

Generally, structure determination of membrane proteins (MPs) is a major challenge due to their amphiphilic nature. Initially, embedded in biological membranes, MPs need to be solubilized with a suitable detergent for further processing. Ideally, this detergent resembles the physiological environment as closely as possible and satisfies with its alkyl chain(s) the apolar requirements, while at the same time its polar head group interacts with the hydrophilic area of the MP. To quickly identify optimal conditions for MPs for structure analysis, a number of GFP-fusion protein approaches were developed over the last five years[17, 18, 19, 20]. Making use of the fluorescence of the GFP, these approaches allow to monitor solubilization, purification, and stabilization of MPs with the ultimate goal to apply the determined parameters to the untagged MP. Given the small number of determined MP structures to-date, the ultimate aim of this pre-crystallization screen is to speed up the otherwise awfully tedious path of identification and production of MPs that have a high chance to crystallize.

1.6. Aim of the thesis

Using the described GFP-fusion protein approach this master thesis was set out with three major goals:

- Identification of bacterial exchangers from thermophiles suitable for structural studies.
- Pre-crystallization screen with the promising candidates to determine the optimal parameters with respect to solubilization, purification, and stabilization.
- Creation of generally applicable tools beneficial for pre-crystallization screens of MPs.

2. Materials & Methods

2.1. GFP-fusion constructs

To efficiently clone a large number of H^+/Ca^{2+} and Na^+/Ca^{2+} exchangers or any other MP, a ligation-independent cloning (LIC) approach was applied. For this purpose, the original pGAPZ vector used for MP expression in *Pichia pastoris* (life technologies, Invitrogen corporation) was modified to obtain C-terminal (LIC3 vector) and N-terminal (LIC4 vector) GFP-fusions. In addition, a Swa I recognition site for the LIC reaction and a PreScission protease cleavage site, LEVLFQG, for subsequent GFP-tag removal was incorporated up- and downstream of the GFP sequence, respectively. Furthermore, the GFP-encoding sequence contained all mutations to create a so-called superfolder GFP (SF-GFP) that displays vastly improved stability and enhanced brightness of the fluorescence signal [21]. For purification purposes, N-terminal (LIC4

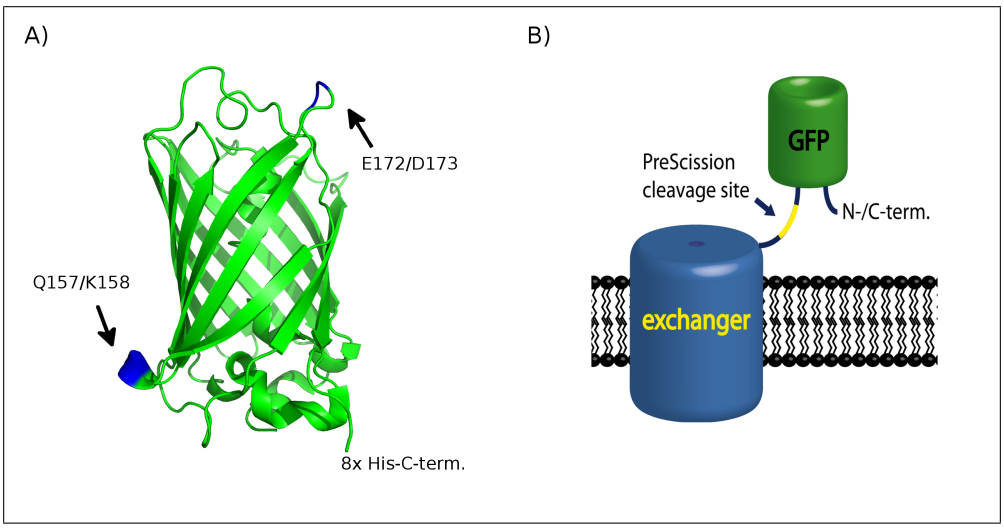

Figure 4: A) Engineering of a Strep-tag into exposed loops of SF-GFP at sites Q157/K158 (LIC3C vector) and E172/D173 (LIC3D vector) with octa-His-tag at the C-terminus. B) N- or C-terminal GFP-fusion constructs with the PreScission cleavage site indicated in yellow.

vector) and C-terminal (LIC3 vector) octa-his-tags were included as well. Later, to further improve sample purity two derivatives of the LIC3 vector were created by introducing a Strep-tag (WSHPQFEK) between Q157/K158 (LIC3C) and E172/D173 (LIC3C) into exposed loops of SF-GFP (Fig. 4).

For the LIC reactions, modified pGAPZ vectors (LIC3, LIC4, and LIC3C) were first linearized with Swa I and then treated with T4 DNA polymerase to produce long sticky ends, required for efficient annealing. Complementary sticky ends were created for the PCR products, encoding the various exchangers. After annealing, the reaction mix was transformed into competent NovaBlue Giga cells (Novagen, Madison, USA) as these cells are capable of closing the remaining nick from the LIC reaction. The transformation mixes were plated on zeocin containing LB plates [22]. Three to four colonies per construct were tested for the presence of the insert by performing minipreps and subsequent restriction enzyme digestions. All sequences of positive clones were sequence-verified (for a detailed LIC protocol see Appendix).

2.2. Bacterial exchangers

Bacterial exchangers were chosen from extremophiles, which thrive in physically or geochemically extreme environments. Adapted to harsh conditions these organisms generally produce thermostable MPs, a property that could be beneficial during MP extraction, purification, and later, especially during crystallization. Initially, exchanger GFP-fusions from ten different extremophilic or thermophilic sources were screened for expression in *Pichia pastoris* X-33. Among those, H^+/Ca^{2+} exchangers from *Thermotoga maritima*, *Deinococcus radiodurans*, and to a lesser extent also from *Pyrococcus furiosus* showed expression levels suitable for structural studies (Fig. 5).

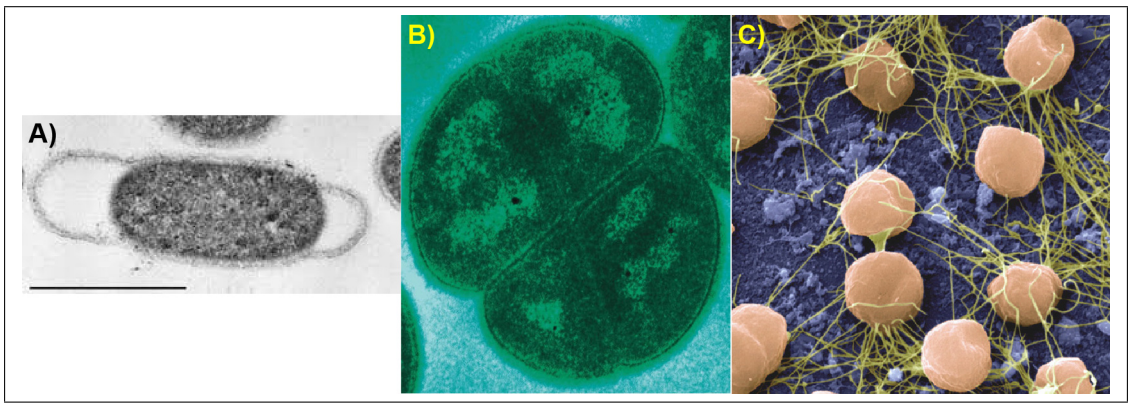

Figure 5: Sources of Ca^{2+} exchangers suitable for structural studies. A) The extremely thermostable bacterium *Thermotoga maritima* is typically found in marine geothermic locations or continental oil fields with resistance to low salinity and an upper growth temperature of 90°C [23]. B) *Deinococcus radiodurans*, one of the most radioresistant organism known that in addition can survive cold, dehydration, vacuum, and acid. These polyextremophilic properties are the reason that *Deinococcus radiodurans* has been listed as the world's most robust bacterium in the Guinness Book Of World Records [24]. C) *Pyrococcus furiosus*, an anaerobic hyperthermophilic archeon with an optimal growth temperature of 100°C [25]. It is predominantly found in the deep sea near hot springs and is resistant to high pressure and elevated salinity.

2.3. Expression trials of GFP-fusions in *Pichia pastoris*

Sequence-verified constructs were linearized by Avr II or Bsp HI and subsequently transformed into the yeast strain *Pichia pastoris* X-33 using electroporation. Transformation mixes were plated on YPDS plates containing 100μg zeocin/ml of agar. Up to 12 colonies per construct were streaked out on a fresh YPDS plate after three to four days. After an additional two days colonies were tested for exchanger expression in 10ml YPD medium. As the GAP promoter on the vector is a constitutive promoter no manual induction was required. Per construct three to four 2ml samples were taken at different optical densities (OD_{600} of 1-8 for mammalian exchangers, OD_{600} of 8-20 for bacterial exchangers). The samples were centrifuged and the pellets were stored at -20°C. For expression analysis, yeast cells were resuspended in breaking buffer (50mM Tris-HCl (pH 8), 10% glycerol, 24.5μl β-mercapto-ethanol, and $\frac{1}{4}$ of a Complete tablet® per 30ml) containing 20mM DDM. After addition of an aliquot of 0.4mm glass beads cells were broken by vortexing twice for 15 seconds. MPs were then extracted for 2h at 4°C and supernatants were analyzed by in-gel fluorescence electrophoresis.

2.4. Pre-crystallization screen of promising exchangers

GFP-fusions of promising exchangers were expressed in 1l of YPD medium until the optimal optical density was reached. The cells were then collected in eight 50ml Falcon tubes. For solubilization tests, cells of a pellet were resuspended in 30ml of breaking buffer and disrupted using a Microfluidizer® M-110P (Microfluidics, Newton, USA). The cell debris was removed by centrifugation at 6000g for 10min and crude membranes were obtained by centrifugation of

the supernatant at 140'000g for 1h using a Beckman 70 Ti rotor.

To screen for a suitable detergent an aliquot of the crude membrane was extracted for 2h with one of the following detergents: n-Dodecyl-β-D-Maltopyranoside (DDM), n-Decyl-β-D-Maltopyranoside (DM), n-Octyl-β-D-Glycopyranoside-8 (β-OG), 6-Cyclohexyl-1-Hexyl-β-D-Maltoside (Cymal-6), and the zwitter-ionic detergent n-Dodecyl-N,N-Di-methylamine-N-Oxide (LDAO) (all from Anatrace, Ohio, USA). Prior to the analysis by Fluorescence Size-Exclusion Chromatography (FSEC) samples were centrifuged at 140'000g for 1h. 500μl of the supernatant was then loaded onto a self-made Superose-6 column (24ml bed volume) and fractions of 150μl were collected in a 96-well microtiter plate. Using a LightCycler® 480 System (Roche, Basel, Switzerland) the fluorescence of the GFP was measured at 20°C with wavelengths of 480 and 510nm for excitation and emission, respectively. The evaluation of the FSEC traces allowed to monitor the solubilization efficiency of different detergents and facilitated an assessment of the aggregation state of the MP GFP-fusions without the need to purify the sample [17]. Using the detergents determined by FSEC, purification protocols were worked out (for details see Appendix).

2.5. Negative-stain and TEM

Carbon-coated copper grids were glow-discharged in a vacuum chamber for 30sec using 500V. Subsequently, 5μl of diluted sample were loaded on a grid and incubated for 1min. The grid was then washed 10 times with water and stained with 5μl of 2% uranyl acetate solution for 20sec. Afterwards, the sample-loaded grids were dried with blotting paper and stored in a petri dish. Transmission Electron Microscopy (TEM) imaging of the grids was performed with a CM-10 (Philips, Dallas, USA) at an acceleration voltage of 80kV.

2.6. PreScission protease preparation for GFP-tag removal

His-tagged PreScission protease (22kD) that specifically cleaves between the glutamine and glycine residues of LEVLFQG was expressed in *E. coli* BL21 (DE3) cells and purified by means of a Ni-NTA affinity column. After concentration of the eluate, aggregates were removed by passing the concentrate over an Amicon concentrator with a 100kD molecular weight cut-off. The final protein concentration was about 0.6mg/ml. For convenience, the PreScission protease was aliquoted and stored at –80°C.

3. Results & Discussion

3.1. Detergent screens of promising bacterial exchangers from thermophiles

Earlier expression trials using in-gel fluorescence analysis revealed suitable expression levels for three Ca^{2+} exchangers from thermophilic organisms, *Thermotoga maritima*, *Deinococcus radiodurans*, and *Pyrococcus furiosus*. To assess solubilization efficiency and the oligomeric state, the three exchanger GFP-fusions were extracted with a number of different detergents and analyzed by FSEC. In order to get a reference, the first FSEC run was performed with eGFP produced in *E. coli* (Fig. 6). Subsequently, the *Thermotoga* exchanger, extracted with 20mM DDM, 20mM DM, and 2mM Cymal-6, was analyzed. The highest solubilization efficiency was achieved with Cymal-6, followed by DDM and DM. In contrast to Cymal-6 and DDM, the peak obtained with DM was slightly shifted towards higher molecular mass. None of the three extractions led to a void peak, indicative of aggregation.

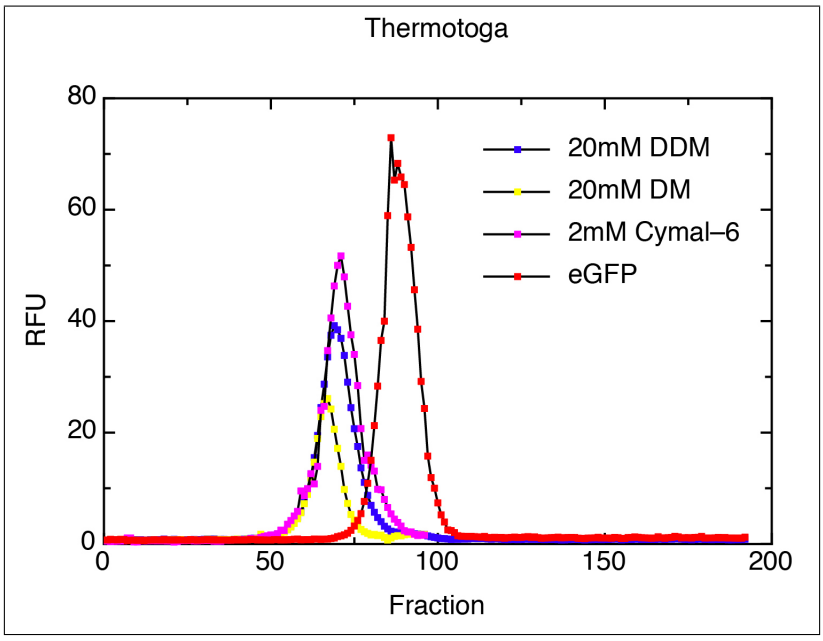

Figure 6: Detergent screen using FSEC technology. The best results were obtained with Cymal-6 (pink) and DDM (blue). The reference, soluble eGFP, is displayed in red.

Similar detergent screens were performed for the *Deinococcus* and the *Pyrococcus* exchangers (Fig. 7). In the case of *Deinococcus* 20mM LDAO and 250mM β-OG were evaluated instead of Cymal-6 (Fig. 7A). The highest extraction efficiencies were obtained with DM and LDAO, however the latter as well as DDM and β-OG displayed as very broad peak that likely reflects a non-monodisperse sample. Although the relative fluorescence units (RFU) cannot be taken as an absolute measure, approximately three-times less *Deinococcus* exchanger could be extracted with respect to the *Thermotoga* exchanger. Finally, presumably due to too low expression levels, extractions of the *Pyrococcus* exchanger were unsuccessful (Fig. 7B). In summary, Cymal-6 and

DDM appear to be reasonable detergents for the *Thermotoga* exchanger, while DM performed best with the exchanger from *Deinococcus*.

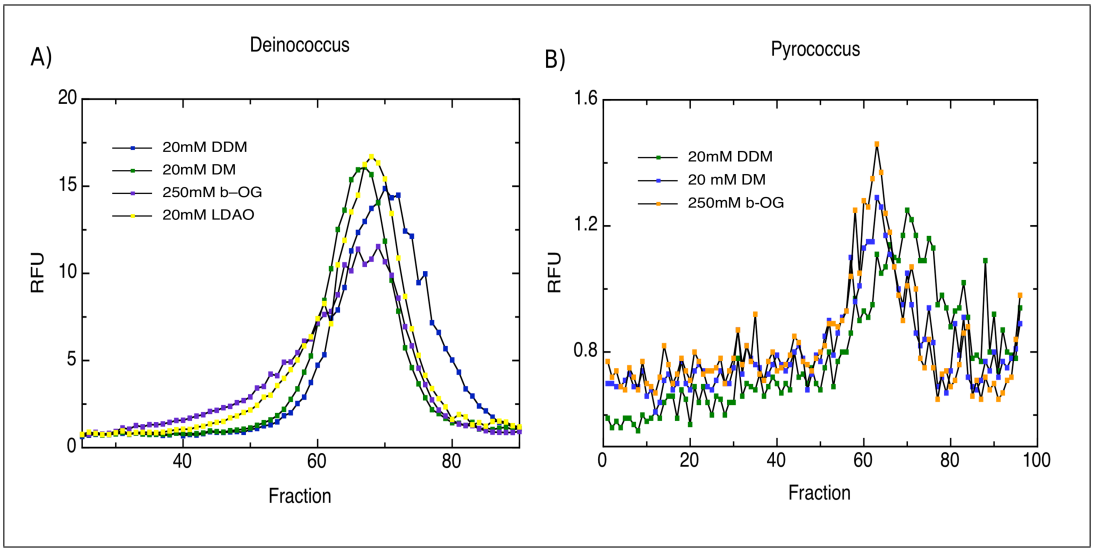

Figure 7: FSEC results for the *Deinococcus* A) and the *Pyrococcus* B) exchanger.

3.2. Purification of *Thermotoga* and *Deinococcus* exchangers

Purification of the *Thermotoga* exchanger was initially achieved using a Ni-NTA and a strep-tactin column. Fig. 8 shows the in-gel-fluorescence analysis and the coomassie-staining of the same gel for the relevant fractions of the two purification steps. The flowthrough of the Ni-NTA column (FT) shows that approximately 30% of the *Thermotoga*-SF-GFP-H_8 construct did not bind to the Nickel beads while the streptactin beads appear to bind the construct rather quantitatively (SFT). Furthermore, compared to the Ni-NTA column the streptactin column concentrates *Thermotoga*-SF-GFP-H_8 substantially. The elution fraction of the Ni-column (NE) shows a main fluorescent band at about 45kD and an additional faint band at around 120kD which could correspond to a trimer of the main band. Coomassie-staining of the same gel revealed additional bands at 37 and 65kD, respectively. While the 37kD band is a contamination that is eliminated by the Strep-tag purification, the 45 as well as the 65kD bands were confirmed by MS analysis to be *Thermotoga*-SF-GFP-H_8. In view of the lacking signal in the in-gel fluorescence analysis the 65kD band probably represents unfolded *Thermotoga*-SF-GFP-H_8. Whether the unfolding of the construct is real or related to the electrophoresis remains to be determined. Taken together, the two purification steps result in an approximately 95% pure sample of *Thermotoga*-SF-GFP-H_8 that however shows two extra minor populations of an unfolded monomeric and probably trimeric state.

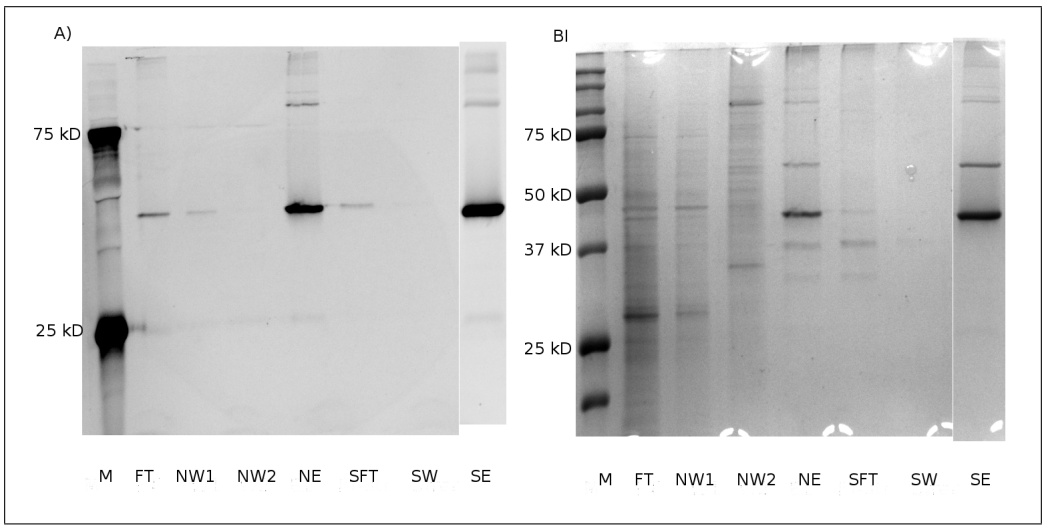

Figure 8: Analysis of Ni-NTA and streptactin column purification steps of *Thermotoga*-SF-GFP-H_8 by means of a 15% SDS-PAGE, displaying the in-gel fluorescence analysis in A) and the coomassie-staining of the same gel in B). M corresponds to the marker, FT is the flowthrough, NW1 and NW2 are the washes, and NE the elution fraction of the Ni column. In contrast, SFT is the flowthrough, SW the wash and SE the elution fraction of the streptactin column.

To speed up purification and to reduce the number of chromatographic steps, single-step purification was attempted using only the streptactin column. The results of this approach are presented in Fig. 9. The purity of the single-step purification is comparable to the two-step purification and makes the Ni-NTA affinity step obsolete for future purifications.

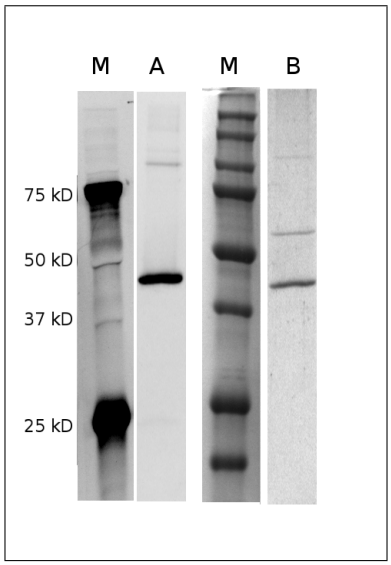

Figure 9: Single-step purification of *Thermotoga*-SF-GFP-H_8 using only a streptactin column. Panel A) displays the in-gel fluorescence analysis while B) shows the same gel stained with coomassie.

The initial His- and Strep-tag purification strategy was also applied to the *Deinococcus* exchanger. For comparison, purified *Thermotoga* and *Deinococcus* exchangers are visualized

by in-gel fluorescence (Fig. 10). The fluorescent bands of the GFP-fusions suggest molecular masses of about 45 and 52kD, respectively. This is approximately 30% less than the calculated masses. Furthermore, the *Deinococcus* exchanger displays a relatively blurry band compared to the sharp band of the *Thermotoga* exchanger which may be attributed to the considerably larger loop regions of the *Deinococcus* exchanger that could potentially adopt a number of different conformational states.

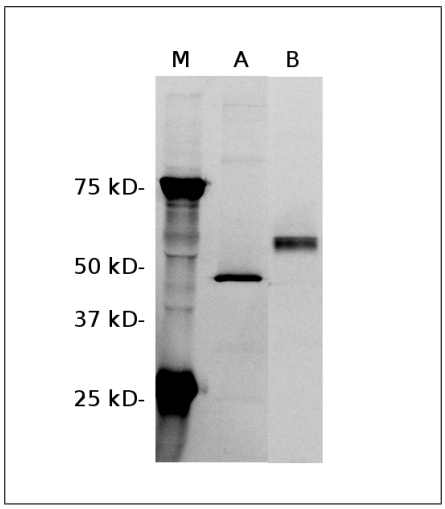

Figure 10: In-gel fluorescence analysis of A) the *Thermotoga* and B) the *Deinococcus* exchanger.

3.3. Coarse yield estimates

To get an estimation for the yield of the purified *Thermotoga* exchanger an analysis of a coomassie-stained SDS-PAGE (Fig. 11) was performed with ImageJ. After applying a "rolling-ball" background correction the area within the turquoise rectangle (Fig. 11A) was integrated and the results were visualized in an one-dimensional plot (Fig. 11B). The plot shows the relative amounts of the folded monomeric *Thermotoga* exchanger (84%) with respect to the unfolded monomeric (12%) and potentially trimeric state (4%).

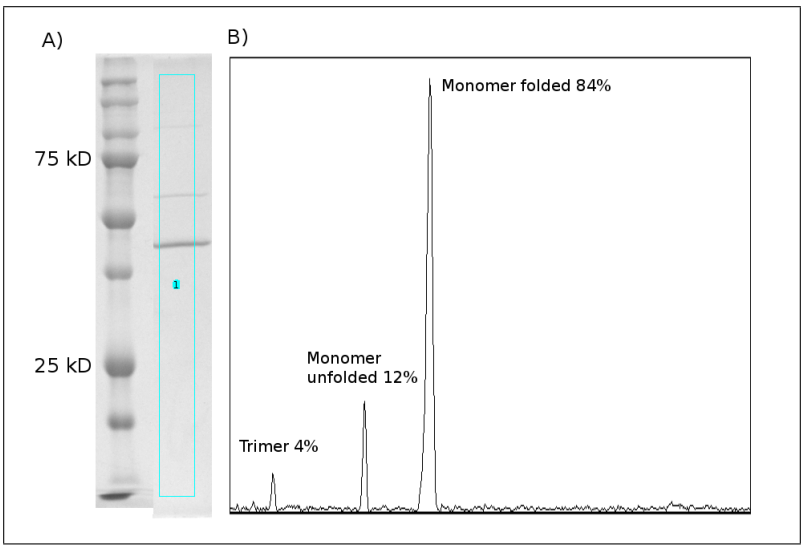

Figure 11: A) Coomassie-stained 15% SDS-PAGE of purified *Thermotoga* exchanger. B) Plot, reflecting the relative amounts of folded monomeric, unfolded monomeric, and potentially trimeric *Thermotoga*-SF-GFP-H_8 as derived from the integration of the rectangle in A).

3.4. Sample upscaling and concentration

Crude membranes of 1l of *Pichia pastoris* culture were solubilized with 20mM DDM and *Thermotoga*-SF-GFP-H_8 was purified as described. Subsequently, the streptactin column elution fractions were concentrated to a volume of 140μl using an Amicon concentrator with a 100kD cut-off. The concentration was approximately 2.5mg/ml or 2.9mg/ml when applying the calculated extinction coefficient ε of 0.876 $(\mathrm{mg/ml})^{-1}\mathrm{cm}^{-1}$. The SDS-PAGE analysis of the concentrate is shown in Fig. 12A. Despite the high protein concentration virtually no impurities or degradation products were visible. However, there might be a limited amount of aggregation. To confirm this assumption FSEC analysis was performed with the concentrated *Thermotoga*-SF-GFP-H_8 sample. Indeed, a small amount of *Thermotoga*-SF-GFP-H_8 is apparently aggregated and elutes as a void peak. A potential problem for the concentration of *Thermotoga*-SF-GFP-H_8 might be the detergent DDM with its low critical micellar concentration (CMC) that is concentrated along with the exchanger. This is supported by dropbox measurements that revealed an increase of the DDM concentration from 0.51mM (3x CMC) to about 30mM (180x CMC) when concentrating the 14ml streptactin column eluate down to 140μl.

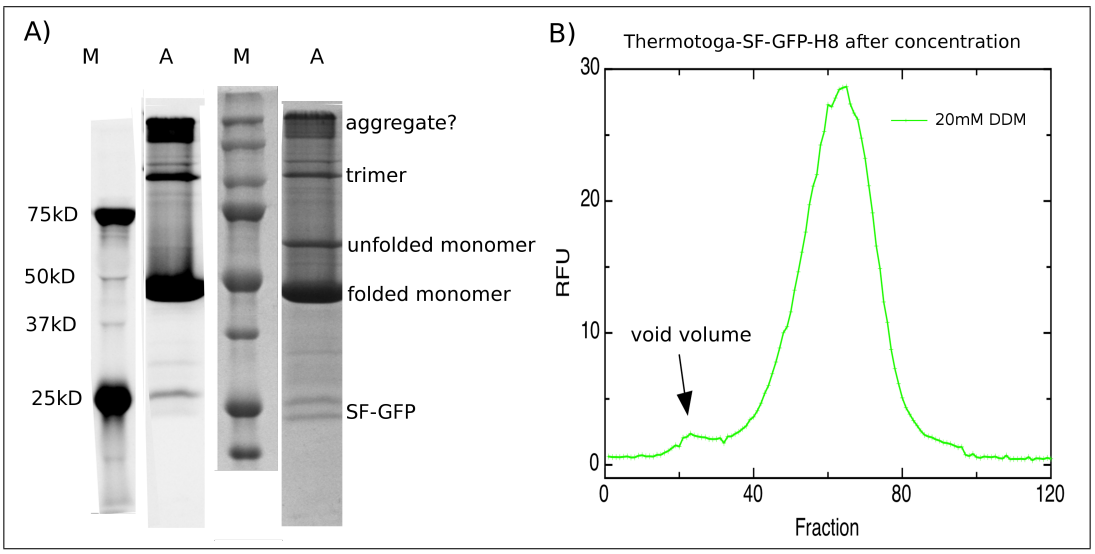

Figure 12: A) SDS-PAGE analysis of the concentrated *Thermotoga*-SF-GFP-H_8 sample. B) FSEC analysis of concentrated *Thermotoga*-SF-GFP-H_8 indicating some very limited aggregation.

3.5. Removal of the GFP-tag

Until now all described experiments were performed with GFP-fusion proteins. However, to get rid off the unfolded monomeric form (Fig. 12A) as well as to obtain a sample that can be used for crystallization the GFP-tag should be preferentially removed. For this purpose, we initially engineered the LEVLFQG recognition sequence for PreScission protease between the C-terminus of the exchanger and SF-GFP (Fig. 4B). Digestion of *Thermotoga*-SF-GFP-H_8 for 4h shows that approximately 90% of the fusion protein is cleaved (Fig. 13). The *Thermotoga* exchanger without the GFP-tag is only poorly stained with coomassie and shows a molecular mass of about 28kD.

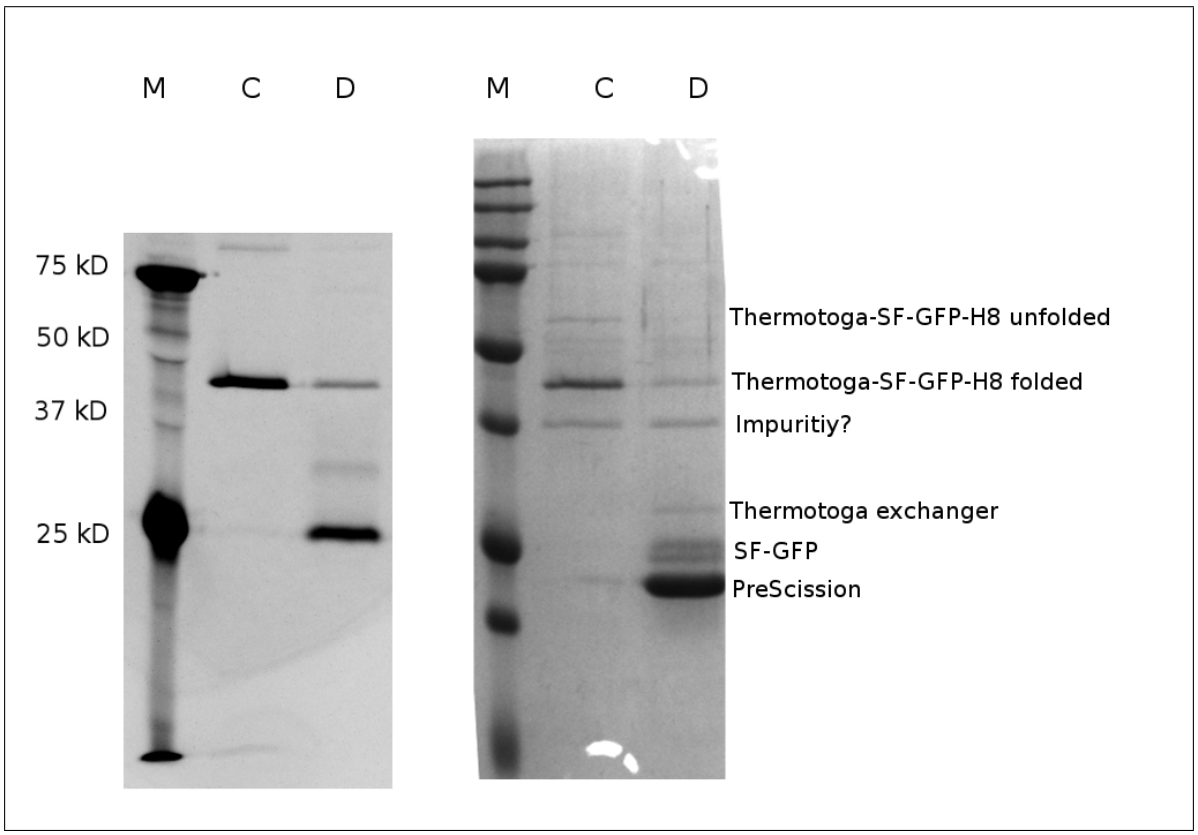

Figure 13: PreScission protease digestion of the *Thermotoga* exchanger. On the left is the in-gel-fluorescence analysis while the coomassie staining of the same gel is presented on the right. M are the marker lanes, C are controls with undigested *Thermotoga*-SF-GFP-H_8, and D are the digestions.

3.6. Assessment of sample homogeneity by electron microscopy

In an attempt to assess the homogeneity of partially purified *Thermotoga* and *Deinococcus* exchangers, EM grids were prepared using uranyl acetate. Various dilutions of the *Thermotoga* and *Deinococcus* exchangers in the determined detergents were examined with the CM-10. In agreement with FSEC pre-crystallization screens, the best results were obtained for the *Thermotoga* exchanger in DDM and the *Deinococcus* exchanger in DM (Fig. 14). While clearly particles with an expected diameter of ∼7nm can be identified, the preparations were far from homogeneous. This lack of monodispersity may be attributed to several factors. First, the samples were only purified by Ni-NTA affinity and a considerable amount of impurities might still have been present. Second, as pointed out before, there are probably three states of the exchangers present in the sample. And third, inhomogeneities might also have arisen from the preparations of the EM grids.

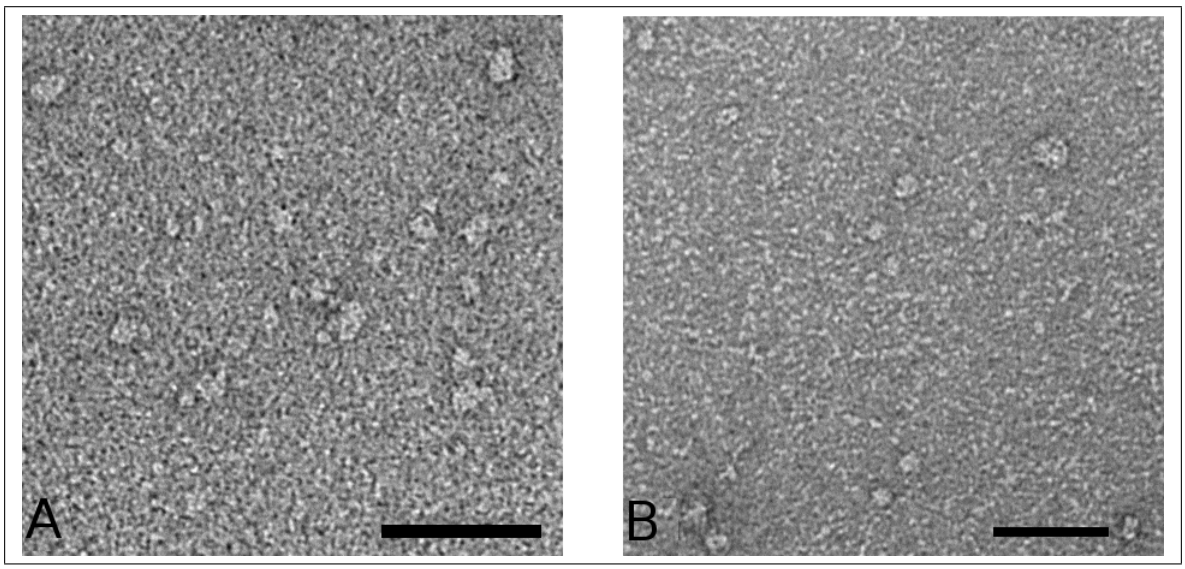

Figure 14: Negative stain analysis of the *Thermotoga* exchanger in DDM A) and the *Deinococcus* exchanger in DM B). The scale bars correspond to 50nm.

4. Conclusions

Using a GFP-fusion approach three bacterial Ca^{2+} exchangers from thermophiles suitable for structural studies were identified. Subsequent FSEC analysis suggested DDM to be a promising detergent for the *Thermotoga maritima* exchanger, while DM looked most promising for an exchanger from *Deinococcus radiodurans*. In contrast, because of the low expression level and/or incompatibilities with the tested detergents solubilization of the *Pyrococcus* exchanger failed. A single-step purification protocol using a Strep-tag engineered into a loop of SF-GFP yielded highly pure (>95%), predominantly monomeric *Thermotoga* and *Deinococcus* exchangers. Inhomogeneities mainly arose from an unfolded monomeric (∼12%)and a probably trimeric (∼4%) state. It was possible to concentrate the *Thermotoga* exchanger to at least 3mg/ml with an acceptable amount of aggregation. Apart from experiments specific to the *Thermotoga* and *Deinococcus* exchangers generally applicable tools were developed and tested. This included the preparation of a His-tagged PreScission protease as well as four new variations of the SF-GFP-tag.

5. Outlook

As there are indications that the GFP-tag is the reason for some aggregation during the concentration as well as for the partial unfolding of the exchanger the GFP-tag probably needs to be removed. Presently, the tag removal is not yet very efficient which may partly be related to the very high DDM concentration in the sample. Prior to setting up crystallization trials these problems need to be resolved. Alternatively, constructs with a Strep-tag instead of a GFP-

tag could be helpful to circumvent problems arising from the GFP-fusion. These Strep-tag constructs could also be very useful for Ca^{2+} uptake assays, based on the dye Fluo-3.

6. Acknowledgements

I thank Dr. Mark Hilge for introducing me into state-of-the-art technologies in molecular biology and biochemistry as well as for wetting my appetite for structural biology. I would like to thank Prof. Henning Stahlberg for the opportunity to carry out my master thesis at his department. I am also very grateful to my co-workers Raphael Küng and Elias Imahorn for good teamwork and an enjoyable time in the lab. Furthermore, I would like to thank Dr. Paul Jenö and Suzanne Moes from the Proteomics Core Facility at the Biozentrum for the professional analysis of exchanger samples using mass spectrometry. Finally, I want to express my gratitude to all the members of C-CINA for a nice atmosphere in the lab.

7. Release and public accessibility

As this master thesis contains unpublished data we would prefer not to release it to the public for the moment.

References

[1] E. Carafoli, "Calcium signaling: a tale for all seasons.," *Proceedings of the National Academy of Sciences of the United States of America*, vol. 99, pp. 1115–22, Feb. 2002.

[2] M. J. Berridge, M. D. Bootman, and H. L. Roderick, "Calcium signalling: dynamics, homeostasis and remodelling.," *Nature reviews. Molecular Cell Biology*, vol. 4, pp. 517–29, July 2003.

[3] X. Cai and J. Lytton, "The cation/Ca2+ exchanger superfamily: phylogenetic analysis and structural implications," *Molecular Biology and Evolution*, vol. 21, pp. 1692–703, Sept. 2004.

[4] D. A. Nicoll, S. Longoni, and K. D. Philipson, "Molecular cloning and functional expression of the cardiac sarcolemmal Na+/Ca2+ exchanger," *Science*, vol. 250, pp. 562–5, Oct. 1990.

[5] Z. Li, S. Matsuoka, L. V. Hryshko, D. A. Nicoll, M. M. Bersohn, E. P. Burke, R. P. Lifton, and K. D. Philipson, "Cloning of the NCX2 isoform of the plasma membrane Na+/Ca2+ exchanger," *The Journal of Biological Chemistry*, vol. 269, pp. 17434–9, July 1994.

[6] D. A. Nicoll, B. D. Quednau, Z. Qui, Y. R. Xia, A. J. Lusis, and K. D. Philipson, "Cloning of a third mammalian Na+/Ca2+ exchanger, NCX3," *The Journal of Biological Chemistry*, vol. 271, pp. 24914–21, Oct. 1996.

[7] P. Kofuji, W. J. Lederer, and D. H. Schulze, "Mutually exclusive and cassette exons underlie alternatively spliced isoforms of the Na+/Ca2+ exchanger," *The Journal of Biological Chemistry*, vol. 269, pp. 5145–9, Feb. 1994.

[8] S. L. Lee and J. Lytton, "Tissue-specific Expression of Na+/Ca2+ exchanger Isoforms," *Journal of Biological Chemistry*, vol. 1, no. 5, pp. 14849–14852, 1994.

[9] B. D. Quednau, D. a. Nicoll, and K. D. Philipson, "Tissue specificity and alternative splicing of the Na+/Ca2+ exchanger isoforms NCX1, NCX2, and NCX3 in rat," *The American Journal of Physiology*, vol. 272, pp. C1250–61, Apr. 1997.

[10] Mark Hilge, "Ca2+ regulation of ion transport in the Na+/Ca2+ exchanger," *Journal of Biological Chemistry article in press.*, 2012.

[11] M. Hilge, J. Aelen, A. Foarce, A. Perrakis, and G. W. Vuister, "Ca2+ regulation in the Na+/Ca2+ exchanger features a dual electrostatic switch mechanism.," *Proceedings of the National Academy of Sciences of the United States of America*, vol. 106, pp. 14333–8, Aug. 2009.

[12] M. Hilge, J. Aelen, and G. W. Vuister, "Ca2+ regulation in the Na+/Ca2+ exchanger involves two markedly different Ca2+ sensors," *Molecular Cell*, vol. 22, pp. 15–25, Apr. 2006.

[13] D. A. Nicoll, L. V. Hryshko, S. Matsuoka, J. S. Frank, and K. D. Philipson, "Mutation of amino acid residues in the putative transmembrane segments of the cardiac sarcolemmal Na+/Ca2+ exchanger," *The Journal of Biological Chemistry*, vol. 271, pp. 13385–91, June 1996.

[14] M. Hilge, J. Aelen, A. Perrakis, and G. W. Vuister, "Structural basis for Ca2+ regulation in the Na+/Ca2+ exchanger," *Annals of the New York Academy of Sciences*, vol. 1099, pp. 7–15, Mar. 2007.

[15] T. Iwamoto, A. Uehara, I. Imanaga, and M. Shigekawa, "The Na+/Ca2+ exchanger NCX1 has oppositely oriented reentrant loop domains that contain conserved aspartic acids whose mutation alters its apparent Ca2+ affinity," *The Journal of Biological Chemistry*, vol. 275, pp. 38571–80, Dec. 2000.

[16] J. Liao, H. Li, W. Zeng, D. B. Sauer, R. Belmares, and Y. Jiang, "Structural insight into the ion-exchange mechanism of the sodium/calcium exchanger.," *Science (New York, N.Y.)*, vol. 335, pp. 686–90, Feb. 2012.

[17] T. Kawate and E. Gouaux, "Fluorescence-detection size-exclusion chromatography for precrystallization screening of integral membrane proteins," *Structure*, vol. 14, pp. 673–81, Apr. 2006.

[18] D. Drew, S. Newstead, Y. Sonoda, H. Kim, G. von Heijne, and S. Iwata, "GFP-based optimization scheme for the overexpression and purification of eukaryotic membrane proteins in Saccharomyces cerevisiae," *Nature protocols*, vol. 3, pp. 784–98, Jan. 2008.

[19] D. Drew, M. Lerch, E. Kunji, D.-J. Slotboom, and J.-W. de Gier, "Optimization of membrane protein overexpression and purification using GFP fusions.," *Nature methods*, vol. 3, pp. 303–13, Apr. 2006.

[20] S. Newstead, H. Kim, G. V. Heijne, S. Iwata, and D. Drew, "High-throughput fluorescent-based optimization of eukaryotic membrane protein overexpression and purification in Saccharomyces cerevisiae," *PNAS*, vol. 104, no. 35, pp. 1–6, 2007.

[21] J.-D. Pédelacq, S. Cabantous, T. Tran, T. C. Terwilliger, and G. S. Waldo, "Engineering and characterization of a superfolder green fluorescent protein," *Nature Biotechnology*, vol. 24, pp. 79–88, Jan. 2006.

[22] C. Aslanidis and P. J. de Jong, "Ligation-independent cloning of PCR products (LIC-PCR)," *Nucleic Acids Research*, vol. 18, pp. 6069–74, Oct. 1990.

[23] "Thermotoga TEM picture." http://www.genomenewsnetwork.org/articles/02_02/extremo_art.shtml. [Online; accessed 20-June-2012].

[24] "Deinococcus picture." http://en.wikipedia.org/wiki/Deinococcus_radiodurans. [Online; accessed 20-June-2012].

[25] "Pyrococcus picture." http://lalecturadelatierra.wordpress.com/2010/11/29/era-eoarcaica/. [Online; accessed 20-June-2012].

A. MP purification protocol

Preparation of crude membranes from 1l of *Pichia pastoris* culture:
Prepare 50ml of ice-cold breaking buffer (50mM Tris-HCl (pH 8), 10% glycerol, 35μl β-mercaptoethanol, and one tablet of Complete® protease inhibitor cocktail (EDTA free) to break cells from 1l of *Pichia pastoris* culture (OD_{600} of about 12) with a heavy-duty microfluidizer. Cover external metal parts with bags filled with ice. Resuspend cell pellet in breaking buffer and keep suspension at 4°C at all times. Break cells for about 10min. Centrifuge broken cells for 15min. at 6000g to remove the cell debris. Subsequently, centrifuge the supernatant for 1h at 140'000g to obtain the crude membranes. Store crude membranes at -80°C.

MP extraction:
Resuspend crude membranes in 30ml of solubilization buffer (20mM Tris (pH 8), 150mM NaCl, and an appropriate amount of detergent, e.g. 20mM of DDM). Extract MPs for 1-2h on a rotator in the cold room. Subsequently, centrifuge for 1h at 140'000g to remove aggregates.

Ni-column:
Incubate supernatant (30ml) with 30ml of pre-equilibrated (B1; 20mM Tris (pH 8), 150mM NaCl and detergent (3x CMC)) Ni-beads on a rotator for 2h in the cold room. Pour slurry into an Econo column and pass the flowthrough three-times over the column. Wash with 30ml of buffer B1 and then with 60ml of buffer B1 containing 25mM imidazole. Elute His-tagged MP with 30ml of B1 containing 500mM imidazole.

Streptactin column:
Incubate Ni-column eluate with 4ml pre-equilibrated (NP: 50mM NaH_2PO_4, 300mM NaCl, adjust pH 8 and detergent (3x CMC)) streptactin beads on a rotator for 1h in the cold room. Pour slurry in an Econo column and pass flowthrough three times over the column. Wash the beads with 36ml of NP buffer. Elute MP with 10ml of NP buffer containing 2.5mM desthiobiotin. Regenerate the streptactin beads with "beads regeneration solution" (50mM NaH_2PO_4, 300mM NaCl, 1mM HABA, adjusted to pH 8) and rinse with NP buffer. Do not use ddH_2O for streptactin beads. Monitor the color change from greyish (loaded), red (regeneration) to white (clean).

B. LIC-cloning protocol

DNA amount calculation:
Use 0.2pmol DNA (inserts and vectors) per LIC reaction applying the formula: #bp DNA x 650 = pg/mol.

DNA type	**[bp]**	**[ng]**
pPICZ LIC3/4 SwaI digested	4127	544
pGAPZ LIC3/4 SwaI digested	3680	486
Thermotoga	930	130
Deinococcus	1220	150
NCX1/NCX2/NCX3	3000	390

T4 DNA polymerase mix:
Vector: 13μl DNA (0.2pmol), 2μl 10xT4 DNA polymerase buffer (NEB2), 1μl 20xBSA, 2μl 25mM d**C**TP, 1μl 100mM DTT and 1μl T4 DNA polymerase (NEB).

Insert: 13μl DNA (0.2pmol), 2μl 10xT4 DNA polymerase buffer (NEB2), 1μl 20xBSA, 2μl 25mM d**G**TP, 1μl 100mM DTT and 1μl T4 DNA polymerase (NEB).

Mix and incubate for 1h at 22°C. Heat inactivate T4 DNA polymerase for 20min at 75°C.

Annealing:
Mix 2.5μl of the T4-treated vector and 5μl of the T4-treated insert. Incubate the mix for 20min at 22°C. Add 2.5μl of 25mM EDTA and incubate for 5min at 22°C.

Transformation:
Mix 10μl of competent NovaBlue Giga cells with 10μl of annealing mix and incubate for 5min on ice. Heat shock the transformation mix for 30sec at 42°C and incubate on ice for 1min. Add 250μl of SOC medium and shake at 37°C for 1h. Plate all cells on a zeocin (25μg/ml) containing LB plate and incubate overnight at 37°C.

Philosophisch-Naturwissenschaftliche Fakultät
der Universität Basel
Dekanat

Erklärung zur wissenschaftlichen Redlichkeit
(beinhaltet Erklärung zu Plagiat und Betrug)

(bitte ankreuzen)
☐ Bachelorarbeit
☒ Masterarbeit

Titel der Arbeit *(Druckschrift)*:
PRECRYSTALLIZATION SCREEN OF NA+/CA2+ EXCHANGERS FROM THERMOPHILIC ORGANISMS

Name, Vorname *(Druckschrift)*: DEVANTAY NICOLAS

Matrikelnummer: 06-050-942

Hiermit erkläre ich, dass mir bei der Abfassung dieser Arbeit nur die darin angegebene Hilfe zuteil wurde und dass ich sie nur mit den in der Arbeit angegebenen Hilfsmitteln verfasst habe.

Ich habe sämtliche verwendeten Quellen erwähnt und gemäss anerkannten wissenschaftlichen Regeln zitiert.

Diese Erklärung wird ergänzt durch eine separat abgeschlossene Vereinbarung bezüglich der Veröffentlichung oder öffentlichen Zugänglichkeit dieser Arbeit.

☒ ja ☐ nein

Ort, Datum: BASEL, JULY 4, 2012

Unterschrift: N. Devantay

Dieses Blatt ist in die Bachelor-, resp. Masterarbeit einzufügen.